



Prediction of Carbamazepine-Succinic Acid Co-Crystal Dissolution in Ethanolic Solution using a Computational Molecular Dynamic Simulation Technique

Nornizar Anuar^{1*}, Noor Sazmira Pauzi¹, Siti Nurul 'Ain Yusop¹, Nik Salwani Md Azmi¹, Syarifah Abd Rahim², Muhammad Fitri Othman¹

¹Faculty of Chemical Engineering, Universiti Teknologi MARA, 40450 Shah Alam, Selangor

²Faculty of Chemical and Natural Resources Engineering, Universiti Malaysia Pahang, Pekan 26300 Pahang, Malaysia

*Corresponding author E-mail: nornizar@salam.uitm.edu.my

Abstract

Carbamazepine (CBZ) is an anti-epileptic Class II drug according to the biopharmaceutical classification system and it forms a co-crystal with succinic acid (SA). The physicochemical properties of co-crystal are of interest since they control how the co-crystal behaves in different environment. In this study, the morphology of carbamazepine-succinic acid (CBZ-SA) co-crystal was predicted by applying the atomic charge calculated from MOPAC and DMol3 while the dissolution behavior of CBZ-SA in ethanol was investigated using dynamic simulation by considering the transport properties of both co-crystal and solvent. The predicted CBZ-SA morphology shows a plate-like shape with the main crystal facet of (1 0 -1), (1 0 1), (1 1 0), (0 1 1), (0 1 0), (2 0 0) and (0 0 2). Attachment energy calculation shows that facet (1 0 -1) is the slowest growing facet having the lowest attachment energy of -27.91 kcal/mol, while facet (0 1 1) is the fastest growing facet with the highest value of attachment energy of -96.74 kcal/mol. The dissolution behavior of CBZ-SA in ethanol was also assessed through the mean square displacement (MSD) and diffusion coefficient calculation, and the result shows that the dissolution of co-crystal first occurs at facet (1 0 1) and last to dissolve at facet (1 1 0). Because the molecular configuration of the molecules at facet (1 0 1) leaves a large gap between molecules that makes it easier for the solvent molecules to penetrate the surface layer and the hydrophilic part of CBZ and succinic acid molecules is exposed to the surface forming hydrogen bond. Calculation of binding energy shows that the interaction of ethanol was more favorable at facet (1 1 0) with the value of -745.631 kcal/mol. The analysis carried out in this work showed that there is a promising relationship between RDF and diffusion coefficient in predicting the diffused molecules from the surface of the facets, as both methods predicted the facets (0 0 2), (2 0 0) and (1 0 1) as among the top three facets dissolved into the ethanol environment. Both MSD and diffusion coefficient also predict that facets (0 1 0) and (1 1 0) are among the last facets dissolved. However, the binding energy calculation does not show any apparent relationship to neither RDF nor diffusion coefficient.

Keywords: Carbamazepine; co-crystallization; dissolution; molecular dynamic simulation; morphology; solubility; succinic acid; surface chemistry.

1. Introduction

Carbamazepine (CBZ) is an active pharmaceutical ingredient (API) used in pharmaceutical industries as an anti-epileptic drug, which belongs to the biopharmaceutics classification system (BCS) class II (low solubility and high permeability) [1]. However, CBZ is practically insoluble in water and has dissolution-limited bioavailability [2]. About 80% of pharmaceutical drugs in powder form have problems with solubility, stability, and flowability [3]; and most of the API drugs are poorly water soluble [4]. Co-crystals production is one of the methods used by pharmaceutical industry to counter the drug solubility problem [5]. Co-crystals comprise of active pharmaceutical ingredients and one or more co-crystal formers, packed together in a unit cell of a crystalline structure [6]. Some commonly used co-formers to produce co-crystals with API are succinic acid, nicotinamide, salicylic acid, adipic acid, fumaric acid, succinic acid, and so on [7]. As an example, carbamazepine-succinic acid cocrystal is formed from carbamazepine and coformer succinic acid. [5, 8, 9]. Dissolution is the first step in the drug absorption process where the drug molecules detach itself from the solid crystal particles

and released into the surrounding gastrointestinal (GI) environment, which makes dissolution rate fundamentally important in designing pharmaceutical dosage form [10]. Nevertheless, the understanding on the molecular dissolution mechanism of solid dispersions remains unclear, despite many well-established reports and extensive pharmaceutical investigation conducted in the past years [10, 11]. The understanding on how the detachment of drug molecules from the crystalline solid phase into the solution is still poor due to the difficulty in experimentally deducing the detachment mechanism at molecular level [10]. Hence, computational methods especially molecular dynamic simulation is an alternative and a powerful tool to help in gaining insight of the mechanism at both atomic and molecular level. It is also able to calculate the physicochemical properties of a substance or a system without costly experiments [11].

In this study, the morphology of carbamazepine – succinic acid (CBZ-SA) cocrystal and the dissolution of the cocrystal were predicted, based on the assessment between the inter- and intramolecular interactions within the cocrystal using a molecular modelling technique. Attachment energy model was used to predict the morphology [12] of CBZ-SA co-crystal. Hartman and

Bennema proposed the attachment energy model based on the period bond chain (PBC) theory [13]. Attachment energy model involves the measurement of energy released due to the addition of a growth slice to growing crystal facet. Attachment energy, E_{att} is calculated as Eq. (1) where E_{latt} is the lattice energy of the crystal and E_{slice} is the energy of growth slice [13]:

$$E_{att} = E_{latt} - E_{slice} \quad (1)$$

Growth morphology can be predicted by assuming that the growth rate is proportional to the absolute value of the attachment energy [13, 14], where the main stable facet with different Miller indices was acquired. Dynamic simulation was used to investigate the dissolution behaviour of co-crystal in solvent, while mean square displacement (MSD) and radial distribution function (RDF) analysis was conducted after a successful dynamic run.

MSD measures the displacement of molecules from its original positional and the MSD data was used to calculate the diffusion coefficient. The diffusion coefficient, D was calculated from the slope of the linear part of the MSD versus t curve using Einstein relation (Eq. 2) where $r_i(t)$ and $r_i(0)$ stand for the coordinates of particle i at time t and initial time, respectively, while $\langle [r_i(t) - r_i(0)]^2 \rangle$ is the mean squared displacement of coordinates [15, 16].

$$D = \frac{1}{6} \lim_{t \rightarrow \infty} \frac{d}{dt} \langle [r_i(t) - r_i(0)]^2 \rangle \quad (2)$$

The radial distribution function (RDF) is also analyzed from the trajectory data. RDF is usually used to investigate specific interactions i.e hydrogen bonding [17]. RDF measures the probability of an atom/molecule found from a reference atom at a distance, r [13] and the number of particles around the central atom is proportional to the volume surrounded by two spheres.

2. Materials and method

2.1. Molecular structures

Carbamazepine-succinic acid (CBZ-SA) co-crystal structures were extracted from the Cambridge Structural Data (CSD) with the reference code of XOBICB. CBZ-SA crystallizes in a monoclinic lattice with space group P2₁/N, with cell parameters of $a = 17.729739 \text{ \AA}$, $b = 5.217281 \text{ \AA}$, $c = 20.753143 \text{ \AA}$, $\beta = 103.35299^\circ$, α and $\gamma = 90^\circ$. CBZ-SA co-crystal is packed with four molecules of carbamazepine (CBZ) and two molecules of succinic acid (SA) in a unit cell (Fig. 1). Both succinic acid molecules are packed in the middle of the crystal lattice structure in between two carbamazepine molecules. Both succinic acid forms hydrogen bond with the hydrophilic part of carbamazepine molecules while the hydrophobic part of CBZ molecules are facing another hydrophobic part of CBZ molecules. The hydrophobic region interactions are only associated with van der Waals interaction.

2.2. Computational methods

Molecular modelling of carbamazepine-succinic acid (CBZ-SA) co-crystal morphology and the dissolution behavior of CBZ-SA in ethanol was simulated using Material Studio (MS) software version 4.4 from Accelrys. The atomic charges were calculated using DMol3 and MOPAC programme, whilst the lattice energy was calculated using attachment energy (EA) method. Molecular dynamic simulation was also carried out with the aim to predict the dissolution behavior of CBZ-SA co-crystal in ethanol, by looking into the mean square displacement (MSD), diffusion coefficient and also the radial distribution function (RDF) data.

2.3. Atomic charge calculation

The calculation for atomic charges was calculated using four methods; i.e. MNDO in MOPAC program; and Mulliken,

Hirshfeld, and Electrostatic potential (ESP) in DMol3, the embedded program in MS. DMol3 applies the density functional theory (DFT) that describes the nature of energy levels of atoms and subatomic particles at the smallest scales. For the atomic charges calculation performed using Mulliken, Hirshfeld, and Electrostatic potential (ESP), the GGA and BLYP functional correlation and DNP basis set were used. The atomic charges calculated using both programmes were then assigned to the CBZ-SA molecular structure.

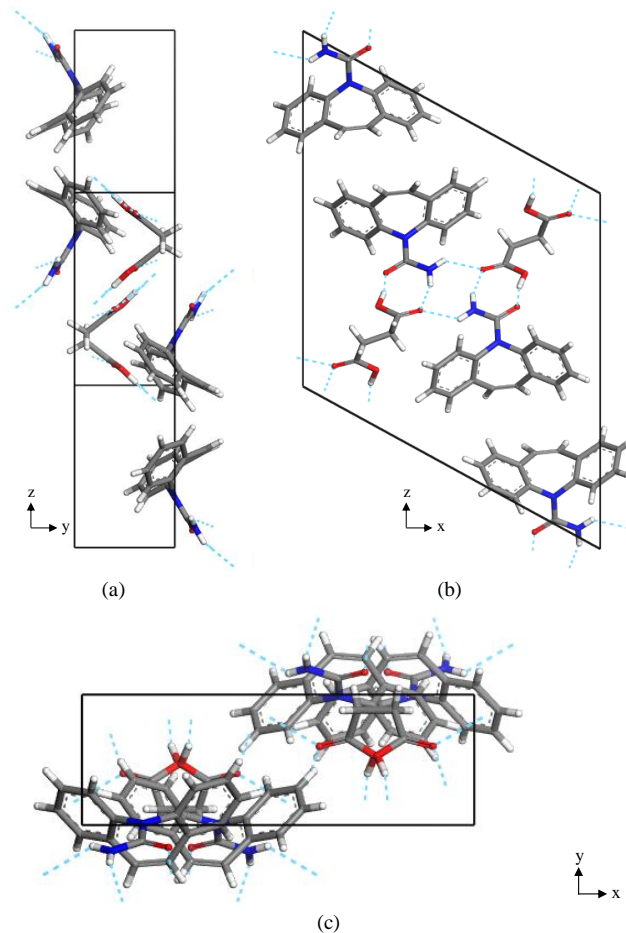


Fig. 1: Molecular structure of CBZ-SA crystal lattice in (a) x-direction, (b) y-direction and (c) z-direction.

2.4. Carbamazepine-succinic acid (CBZ-SA) co-crystal morphology prediction

The charged CBZ-SA molecular structure was then subjected to two stages of geometry optimization using an embedded module in MS prior to morphology prediction. The first stage was to optimize the molecular configuration by keeping the torsion angle and the conformation of the molecules fixed. The second stage was to minimize the energy where all molecules were allowed to move in the system. Crystal growth morphology prediction was conducted using different types of forcefields i.e COMPASS, Dreiding, pcff, Universal, and cvff while Ewald and atom based summation methods were used respectively for electrostatic and van der Waals calculation. Different crystal morphology was produced and the most similar morphology as well as the closest lattice energy to the experimental data was chosen to be used for the dissolution behaviour investigation.

Every facet of the predicted morphology of CBZ-SA co-crystal was cleaved and extended to a 3D periodic superstructure, where the cell was extended to 3 times repetition in U or V direction depending on the configuration of the molecules on the chosen facet. Vacuum slab with the thickness of 55 \AA was built above the crystal surface, to remove the additional free boundaries effect on the structure.

2.5. Construction of 3D periodic structures of ethanol

Ethanol molecule was constructed using the sketching tools available in MS. The structure underwent geometry optimization and minimization energy procedures using Dreiding force field. Then, a cell containing 100 molecules of ethanol was built using Amorphous Cell module. The size of ethanol cell was constructed based on the length and width of the CBZ-SA crystal slab. Then, the ethanol molecules were inserted into the vacuum slab containing CBZ-SA supercell crystal surface.

2.6. Geometry optimization of the periodic system.

For this process, the crystal surface supercells were kept constraint, whilst the ethanol molecules were allowed to move freely for geometry optimization. The system was subjected to geometry optimization using the same forcefield as the morphology of the CBZ-SA co-crystal used. In this case, Dreiding forcefield and current charges were used to maintain the charges from previous calculation. Atom based calculation was selected for the electrostatic and van der Waals summation method. This process sought to find the geometry of a particular arrangement of the atoms where the total energy of the system was reduced to a minimum.

2.7. Molecular dynamics run for dissolution assessment for the periodic systems

Dynamic simulation was conducted after geometry optimization. For dynamic simulation, the first upper layer of the CBZ-SA crystal was unconstrained to allow the crystal to move freely and interact with the ethanol molecules while the two bottom layer remain constrained. Dynamic simulation was conducted for 20 ps with medium quality, 1 fs time step and the frame output was recorded for every 100 steps. Berendsen thermostat was used to control the temperature and NVT (constant number of molecules, constant volume and constant temperature) ensemble was chosen. Dreiding forcefield with atom based calculation was used for both the electrostatic and van der Waals summation method.

2.8. Binding energy

The binding energy, $E_{binding}$ was calculated using Equation 3 [13], where E_{min} is the total energy of solvent layer and the crystal face energy, E_{surf} is the energy of the crystal facet and E_{solv} is the energy of solvent layer.

$$E_{binding} = E_{min} - E_{surf} - E_{solv} \quad (3)$$

3. Results and discussions

3.1. Carbamazepine-succinic acid (CBZ-SA) co-crystal morphology

Crystal morphology of CBZ-SA co-crystal was predicted using different charge sets and forcefield, producing different sets of lattice energy, E_{latt} . Lattice energy is sensitive to the charge sets and forcefields used in the simulation [13]. Based on the values shown in Table 1, this seems to be the case as the lattice energy calculated varies between -110.2 and -558.0 kcal/mol, depending on the forcefield and atomic charges assigned. Most of the morphology predicted by the combination of forcefield and atomic charges shows a plate-like shape except for the morphology predicted using Hirshfeld charges with COMPASS and Dreiding forcefields, where they show an elongated hexagonal shape with a thicker appearance. Based on the assessment of the predicted CBZ-SA morphology, it was concluded that the morphology with Dreiding forcefield using the atomic charge from Hirshfeld calculation, with lattice energy of -145.8 kcal/mol is the most similar to the experimental morphology of CBZ-SA, as reported by Rahim et al. [7]. The comparison of the predicted and experimental CBZ-

SA morphology is depicted in Fig. 2. The predicted CBZ-SA morphology shows a plate-like shape with 18 facets. From Fig. 2, the largest crystal surface is dominated by facets (1 0 -1), (-1 0 1), followed by facets (-1 0 -1) and (1 0 1) while facets (1 -1 0), (1 1 0), (-1 -1 0), (-1 1 0), (0 1 1), (0 1 1), (0 -1 -1), (0 1 -1), (0 -1 0), (0 1 0), (0 0 2), (2 0 0), (-2 0 0) and (0 0 2) are the minor facets for CBZ-SA co-crystal. Dominant crystal surfaces usually are the slow growing facets and they are the most morphologically important facets [13, 18, 19].

Table 1: Predicted lattice energy of CBZ-SA using different forcefield and atomic charges set

Forcefield	Charges	E_{latt} (kcal/mol)
COMPASS	MNDO	-52.69
	Mulliken	-65.02
	Hirshfeld	-37.77
	ESP	-74.03
Dreiding	MNDO	-123.56
	Mulliken	-185.99
	Hirshfeld	-48.60
	ESP	-173.38
Universal	MNDO	-54.31
	Mulliken	-60.27
	Hirshfeld	-45.25
	ESP	-52.87
cvff	MNDO	-47.15
	Mulliken	-44.29
	Hirshfeld	-36.74
	ESP	-62.33
pcff	MNDO	-50.33
	Mulliken	-58.76
	Hirshfeld	-38.39
	ESP	-56.75

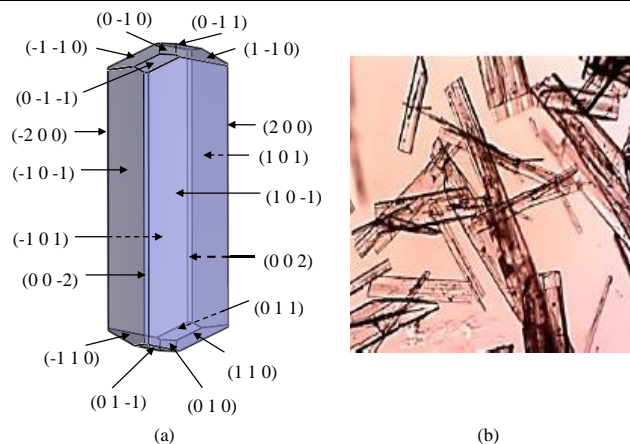


Fig. 2: (a) The predicted morphology of CBZ-SA co-crystal and (b) experimental morphology of CBZ-SA co-crystal [7].

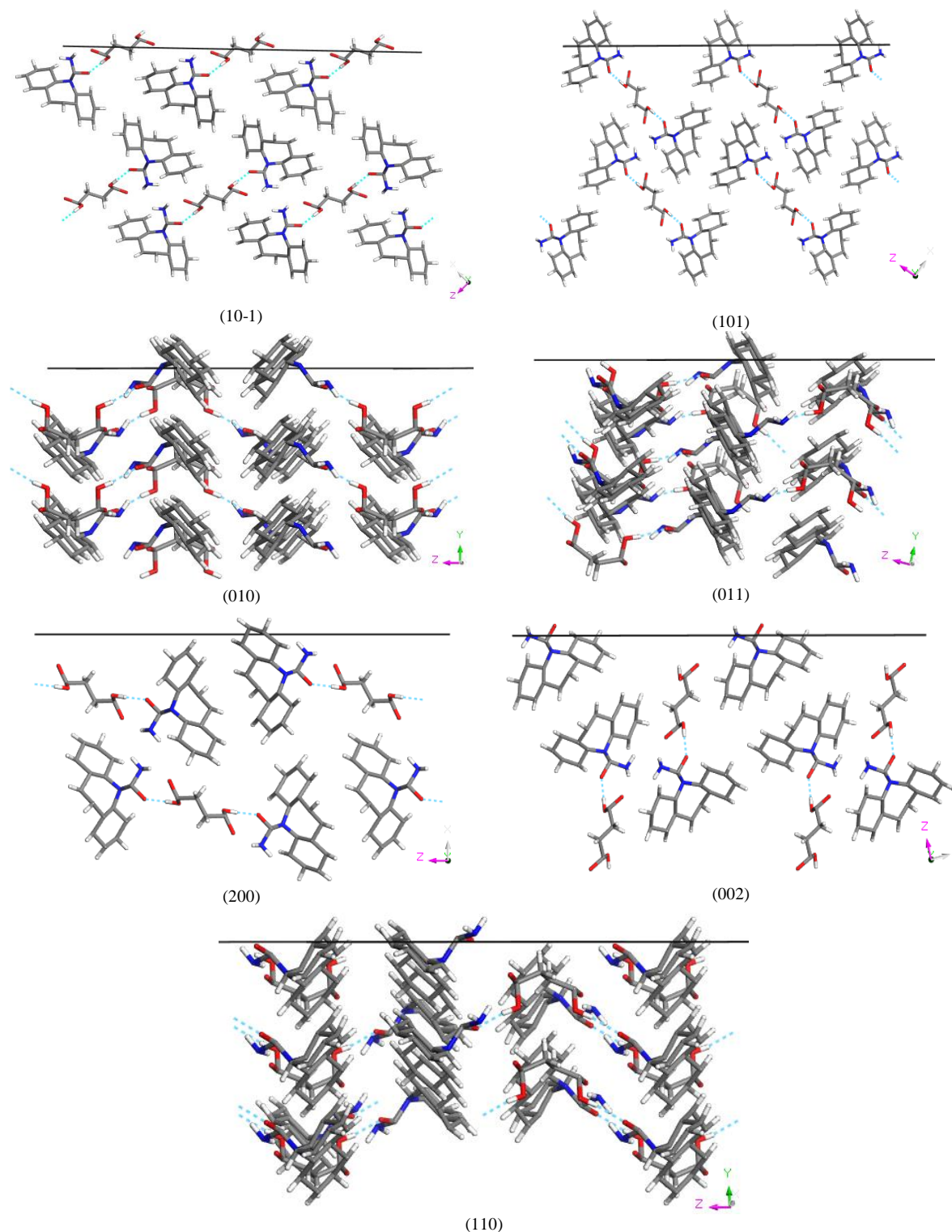
Table 2 shows the predicted parameters for 7 dominant crystal facets, which comprise of facets (1 0 -1), (1 0 1), (0 0 2), (2 0 0), (0 1 0), (0 1 1) and (1 1 0). The results show that facet (1 0 -1) has the highest interplanar distance, $d_{10-1} = 14.929$, while facet (1 1 0) has the lowest interplanar distance, $d_{110} = 4.994$. These indicate that facet (1 0 -1) is morphologically the most important facet of CBZ-SA crystal. The dominating facet (1 0 -1) also has the lowest attachment energy of -27.9 kcal/mol where the growth was the slowest, while minor facet (0 1 1) has the highest attachment energy of -96.7 kcal/mol. Slice energy values depend on the attachment energy where higher slice energy indicates a low absolute attachment energy and the facet will be morphologically important [20].

Slice energy is the measure of energy released when a growth layer is formed, and hence it implies that the more negative the energy, the more energy is being released. From Table 2, facet (1 0 -1) has the highest slice energy of -117.9 kcal/mol and is the most morphologically important crystal facet.

Table 2: Parameters of main crystal facets of CBZ-SA co-crystal.

Crystal facet	Multiplicity	d-spacing	Attachment energy (kcal/mol)	Slice energy (kcal/mol)
(1 0 -1)	2	14.929	-27.907	-6.898
(1 0 1)	2	11.835	-43.080	-1.840
(0 0 2)	2	10.096	-53.723	1.707
(2 0 0)	2	8.625	-43.226	-1.792
(0 1 0)	2	5.217	-93.649	15.016
(0 1 1)	4	5.051	-96.738	16.046
(1 1 0)	4	4.994	-91.338	14.246

The surface chemistry of main crystal facets of CBZ-SA is shown in Fig. 3. The large dominating facet (1 0 -1) with the lowest attachment energy and highest slice energy was built with succinic acid (SA) lining the surface of CBZ-SA co-crystal with half of its molecular structure facing upward. Both the OH and =O of the succinic acid provide an excellent hydrogen bonds binding sites with ethanol. Nonetheless, nitrogen atom of amine group in CBZ also can be a hydrogen bonding site for OH of ethanol. Meanwhile, the second largest crystal facet (1 0 1) is built with the hydrophobic part of the molecular structure protruding upward which

**Fig. 3:** Molecular orientation of CBZ-SA at the main crystal facet

comes from the aromatic amine ring of carbamazepine (CBZ) molecule. This may mean that the van der Waals interaction, a

weak interaction dominates the crystal surface, making it difficult for attachment of molecule to occur. Facet (0 0 2) has the CBZ molecules at the surface with the NH_3 and $\text{C}=\text{O}$ protruding upward while for (1 1 0) facet, even though there is NH_3 and $\text{C}=\text{O}$ groups protruding upwards, there is also hydrophobic ring of CBZ molecules at the surface. For facets (2 0 0) and (0 1 0), hydrogen bonding is observed at the surface and this increases the chances of attachment to occur. Hydrogen bonding is the most important intermolecular interaction in co-crystal design due to its strength, directionality, and universal occurrence in drug-like molecules where most co-crystals formed are linked by hydrogen bonding [21].

3.2. Dissolution and transport properties of CBZ-SA in ethanol solvent

Molecular dynamic simulation was performed to model the effect of ethanol on the CBZ-SA co-crystal morphology. It provides a better understanding to investigate the interactions of crystal surface with the solvent by observing the interaction between solvent and crystal molecules in both atomic and molecular level. The assessment of the dissolution behavior of CBZ-SA co-crystal in ethanol was carried out to study the interaction between crystal surface and ethanol solvent. The surface of the CBZ-SA crystal

crystal inside the vacuum slab for 20 ps using dynamic simulation. After a successful dynamic simulation, the data was extracted and analysis of the trajectory data was conducted. The visual observation of CBZ-SA co-crystal interaction with ethanol at the interface of facets (1 0 -1) and (1 1 0) is shown in Fig. 3. The ethanol molecules are presented in smaller stick size than CBZ and succinic acid molecules for clearer identification purposes.

The colors for different atoms are as follow: red signifies the oxygen atoms, blue is for nitrogen atoms, grey is for carbons and white is for hydrogen atoms. Fig. 4 shows the facets after dynamic simulation, at 20 ps, in which hydrogen bonds are formed between ethanol and the crystal surface molecules, for both facets. At facet (1 0 -1), the succinic acid lining at the surface of the facet was observed to be detached from the bulk crystal surface and 'moves' into the solvent phase. The detachment of CBZ or SA molecules from facet (1 1 0) is not visible, probably due to the arrangement of the molecules on the crystal facet. The restricted movement of molecules at facet (1 1 0) also can be attributed to the strong hydrogen bonding of CBZ and SA molecules within the crystal structure, which makes it harder to be detached to the solvent environment.

Trajectory data from the successful dynamic simulation was obtained and analyzed to determine the transport properties of the crystal surface. Seven main crystal facets were selected and analyzed for the mean square displacement (MSD) (Fig. 5). From the

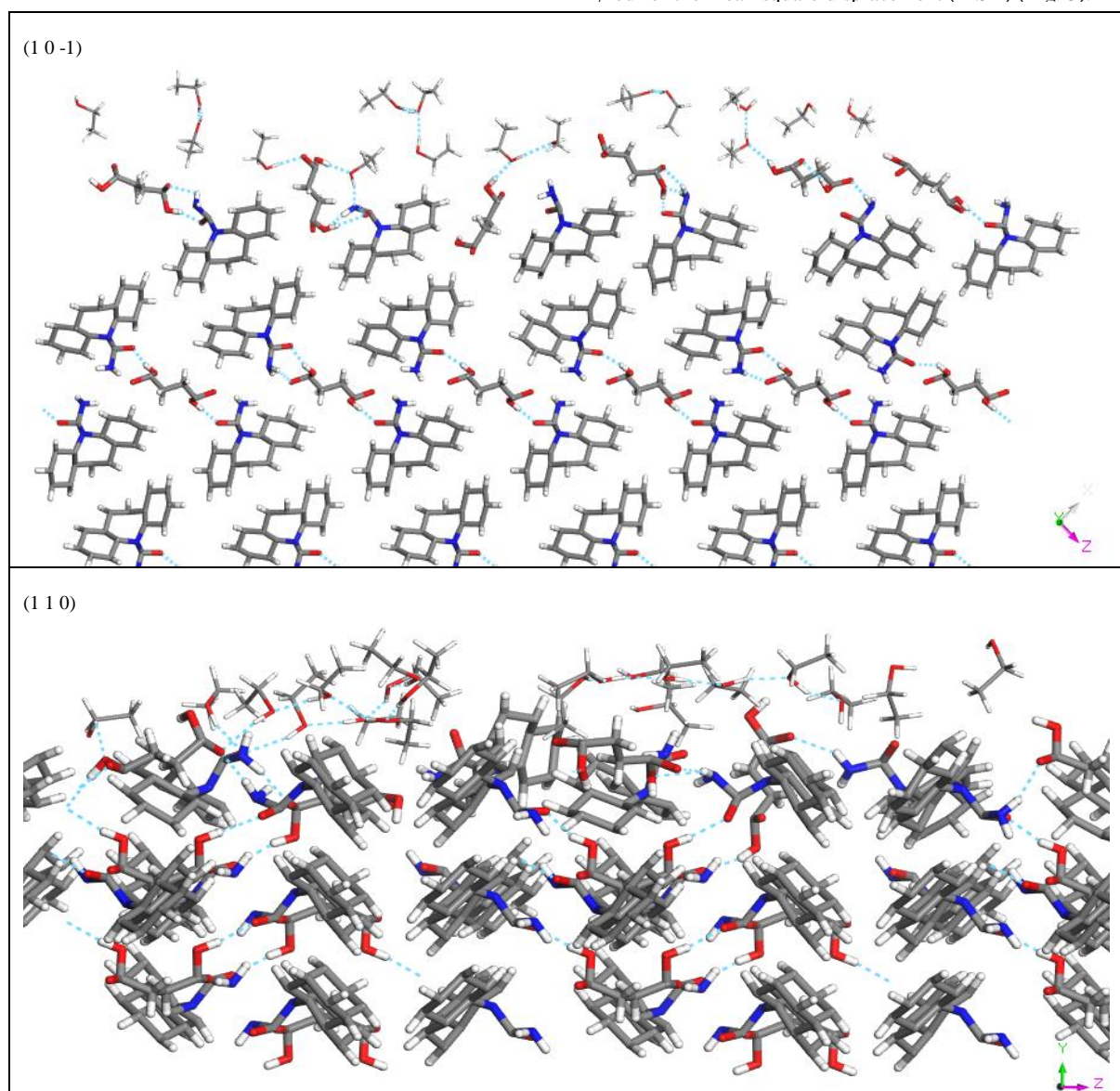


Fig.4: Interaction of CBZ-SA co-crystal facet (1 0 -1) and (1 1 0) after dynamic simulation at 20 ps.

was cleaved and extended to a 3D periodic superstructures prior to building the vacuum slab. Ethanol interacted with CBZ-SA co-

the trend of the MSD curve, it can be seen that the motion behavior of the crystal surface differs as the time increases. MSD curves

show a good linearity at time < 10 ps and the linearity of some of the graph starts to become poor after 10 ps. Similar observation was reported by Zeng et al. [22] where different slope and linearity were observed in the same MSD graph. At time < 1 ps, all facets show similar linear trend, and hence the same line slope and this indicates that the molecules of all facets moves at the same rate and the same frequency. After 1 ps, the movement of the molecules starts to differ depending on the crystal facet where there are changes in the motion between 1 ps and 10 ps. At time 1 ps to 10 ps, the slope of the MSD curves decrease compared to at time < 1 ps, but with apparent difference of slopes for each facets. Higher diffusion slope indicates higher displacement increment and hence stronger movement of molecules [23]. This may be caused by the interaction with the ethanol molecules where the solvent moves closer to the surface of the crystal as depicted in Fig. 3. The diffusion coefficient, D of the crystal surface from time 1 ps to 10 ps was calculated from the slope of the MSD curve and the Einstein relation (Eq. 2) and tabulated in Table 3. The results from Fig. 5 and the values of D calculated in Table 3, show the diffusion coefficient of facet $(1\ 0\ 1) > (2\ 0\ 0) > (0\ 0\ 2) > (0\ 1\ 1) > (1\ 0\ -1) > (0\ 1\ 0) > (1\ 1\ 0)$, and the result indicates that the molecules of facet $(1\ 0\ 1)$ are the first to diffuse to ethanolic solvent environment, followed by the molecules of facet $(2\ 0\ 0)$ and the rest of the molecules following the order above. This result also supports the findings in Fig. 3, in which the visual observation shows that the detachment of the molecules of facet $(1\ 0\ -1)$ are much visible than $(1\ 1\ 0)$. From Fig. 4, most of the MSD curves experience changes in the slope after 10 ps. Some of the facets, such as $(0\ 1\ 1)$ and $(1\ 1\ 0)$ retain the frequency of the motion of molecules as no change in the slopes detected. However facets $(1\ 0\ 1)$, $(2\ 0\ 0)$, $(0\ 0\ 2)$ and $(0\ 1\ 0)$ experience an increase in slope with poor linearity while facet $(1\ 0\ -1)$ experienced a decrease in slope.

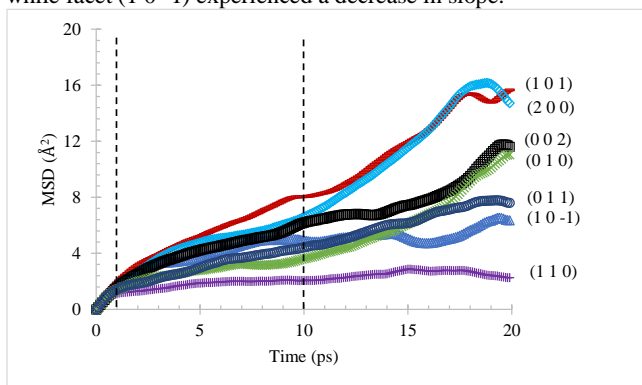


Fig. 5: Motion behavior of main CBZ-SA crystal facet from mean square displacement (MSD) at different time.

Table 3: Diffusion coefficient (D) of main CBZ-SA crystal facet at time 1 ps to 10 ps.

Facet	$D \times 10^{-10}$ (m^2/s)
$(1\ 0\ -1)$	5.40
$(1\ 0\ 1)$	10.91
$(2\ 0\ 0)$	7.87
$(0\ 0\ 2)$	7.32
$(1\ 1\ 0)$	1.78
$(0\ 1\ 0)$	3.37
$(0\ 1\ 1)$	5.62

Radial distribution function (RDF) analysis was also conducted to investigate the structural changes for the molecules in the system. The RDF analysis of different facets is shown in Fig. 6. For all facets, no peaks at radius 3.5 Å was observed. In fact, the first peak for the RDF curve appears at $r > 10$ Å. This shows that there is no hydrogen bond found since hydrogen bond can only be found at $r < 3.5$ Å while the peak found outside of 3.5 Å radius is due to van der Waals and Coulomb interactions [22, 24]. This also could indicate that the RDF analysis measures the detachment of molecules from its crystal lattice of the respective facets. The first peak for facet $(1\ 1\ 0)$, $(0\ 1\ 0)$, $(0\ 1\ 1)$, $(1\ 0\ 1)$, $(1\ 0\ -1)$, $(2\ 0\ 0)$, $(0\ 0\ 2)$ can be found at radius 11, 12, 13, 28, 39, 43 and 49 Å respectively. This means that facet $(1\ 1\ 0)$ is the closest to the reference

atom and the respective peak indicates the first atom/molecule found from the reference atom. Thus, from the analysis, it can be concluded that the diffusion of molecules from the facets is in the following order: $(0\ 0\ 2) > (2\ 0\ 0) > (1\ 0\ -1) > (1\ 0\ 1) > (0\ 1\ 1) > (0\ 1\ 0) > (1\ 1\ 0)$.

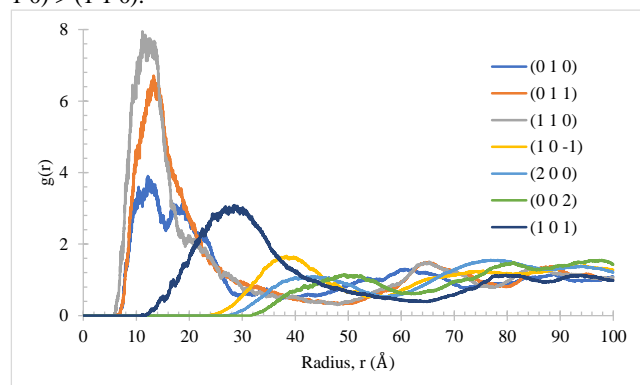


Fig. 6: Radial distribution function (RDF) of main crystal facet of CBZ-SA.

3.3. Binding energies and the solvent effect on CBZ-SA co-crystal morphology

Binding energy can be defined as the minimum amount of energy needed to overcome the forces holding the molecules together within its crystal lattice. In this study, binding energy was calculated to observe an interaction between crystal facet and solvent molecule, which is between CBZ-SA co-crystal facet molecules and ethanol molecules. The binding energies normally focus mainly on the formation of hydrogen bonds which is polar interactions and also van der Waals forces between crystal faces and ethanol. A greater value of interaction energies or binding energies indicates that the interaction between crystal faces and solvent is stronger [24] and hence, more energy is required to separate the molecules from its component parts.

The binding energy of the main facet was calculated using Eq. (3) and tabulated in Table 4. From Table 4, all binding energies show negative values, indicating the adsorption of solvent onto the crystal surface is exothermic and thermodynamically favorable [13]. Negative values of binding energies show that the crystal facet and ethanol molecules are having an attractive interaction. From the results, the value of binding energy was observed to be higher at facet $(1\ 1\ 0) > (0\ 0\ 2) > (0\ 1\ 0) > (0\ 1\ 1) > (1\ 0\ 1) > (1\ 0\ -1) > (2\ 0\ 0)$ which implies stronger interaction between solvent and molecules of the facets. The ability of ethanol molecules to be adsorbed onto the surface of CBZ-SA co-crystal also becomes stronger and hence could be an indication that the possibility of the detachment of the facet molecules to occur.

Table 4: Binding energy for main CBZ-SA co-crystal facets.

Facet	$E_{\text{minimized}}$ (kcal/mol)	E_{surface} (kcal/mol)	E_{solvent} (kcal/mol)	E_{binding} (kcal/mol)
$(1\ 1\ 0)$	-192.644	745.631	-192.644	-745.631
$(0\ 0\ 2)$	-89.115	713.524	-89.115	-713.524
$(0\ 1\ 0)$	-181.698	712.696	-181.698	-712.696
$(0\ 1\ 1)$	-107.877	712.040	-107.877	-712.040
$(1\ 0\ 1)$	-92.835	577.328	-92.835	-577.328
$(1\ 0\ -1)$	-199.91	537.951	-199.910	-537.951
$(2\ 0\ 0)$	-109.098	491.648	-109.098	-491.648

4. Conclusion

The crystal morphology of CBZ-SA and the main crystal facet was successfully predicted using the attachment energy model. The predicted crystal morphology was dominated by seven crystal facets of $(1\ 0\ -1)$, $(1\ 0\ 1)$, $(2\ 0\ 0)$, $(0\ 0\ 2)$, $(1\ 1\ 0)$, $(0\ 1\ 0)$, $(0\ 1\ 1)$. The RDF analysis has shown that the possibility of the molecular detachment from their facets is in the following order: $(0\ 0\ 2) > (2\ 0\ 0) > (1\ 0\ -1) > (1\ 0\ 1) > (0\ 1\ 1) > (0\ 1\ 0) > (1\ 1\ 0)$. The diffusion

coefficients, Ds of facets are arranged in the following order: (1 0 1) > (2 0 0) > (0 0 2) > (0 1 1) > (1 0 -1) > (0 1 0) > (1 1 0), which showed the most possible molecules of the facet diffused from the facet lattice to the ethanol environment. Meanwhile, the binding energy calculated shows that facet (1 1 0) has the highest affinity for ethanol interaction and hence slower growth rate followed by facets (0 0 2), (0 1 0), (0 1 1), (1 0 1), (1 0 -1) and (2 0 0). The analysis carried out in this work showed that there is a promising relationship between RDF and diffusion coefficient in predicting the diffused molecules from the surface of the facets, as both methods predicted the facets (0 0 2), (2 0 0) and (1 0 1) as among the top three facets dissolved into the ethanol environment. Both MSD and diffusion coefficient also predict that facets (0 1 0) and (1 1 0) are among the last facets dissolved. However, the binding energy calculation does not show any apparent relationship to neither RDF nor diffusion coefficient.

Acknowledgement

The authors would like to express their gratitude to the ministry of higher education, Malaysia for funding this work which was carried out at Universiti Teknologi MARA. This work was funded by research grant 600-RMI/MyRA 5/3/BESTARI (023/2017

References

- [1] Ali S, Velaga S, & Jouyban A (2014), Solubility of carbamazepine, nicotinamide and carbamazepine–nicotinamide cocrystal in ethanol–water mixtures. *Fluid Phase Equilibria* 363, 97–105.
- [2] Tian F, Sandler N, Aaltonen J, Lang C, Saville DJ, Gordon KC, Strachan CJ, Rantanen J & Rades T (2017), Influence of polymorphic form, morphology, and excipient interactions on the dissolution of carbamazepine compacts. *Journal of Pharmaceutical Sciences* 96, 584 – 594.
- [3] Vadlamudhi MK & Dhanaraj S (2017), Significance of excipients to enhance the bioavailability of poorly water-soluble drugs in oral solid dosage forms: a review. *IOP Conference Series: Materials Science and Engineering*, 263, 022023
- [4] Cascone, S (2017), Modeling and comparison of release profiles: effect of the dissolution method. *European Journal of Pharmaceutical Sciences* 106, 352–361
- [5] Ab Rahman F, Abd Rahim S, Tan CC, Low SH & Ramle NA (2017), Carbamazepine-fumaric acid and carbamazepine-succinic acid co-crystal screening using solution based method. *International Journal of Chemical Engineering and Applications* 8, 136 – 140
- [6] Liu M, Hong C, Yao Y, Shen H, Ji G, Li G, & Xie Y (2016), Development of a pharmaceutical cocrystal with solution crystallization technology: Preparation, characterization, and evaluation of myricetin-proline cocrystals. *European Journal of Pharmaceutics and Biopharmaceutics* 107, 151–159
- [7] Rahim SA, Rahman FA, Nasir ENEM & Ramle NA (2015), Carbamazepine co-crystal screening with dicarboxylic acids co-crystal formers. *International Journal of Chemical and Molecular Engineering* 9(5), 442-445.
- [8] Fuliş A, Vlase G, Vlase T, Şuta L-M, Şoica C & Ledeti I (2015), Screening and characterization of cocrystal formation between carbamazepine and succinic acid. *Journal of Thermal Analysis and Calorimetry* 121, 1081 – 1086
- [9] Ullah M, Hussain I & Sun CC (2016), The development of carbamazepine-succinic acid cocrystal tablet formulations with improved in vitro and in vivo performance. *Drug Development and Industrial Pharmacy* 42, 969-976
- [10] Gao Y & Olsen KW (2013), Molecular dynamics of drug crystal dissolution: simulation of acetaminophen form I in water. *Molecular Pharmaceutics* 10, 905 – 917
- [11] Chan T & Ouyang D (2018), Investigating the molecular dissolution process of binary solid dispersions by molecular dynamics simulations. *Asian Journal of Pharmaceutical Sciences* 13, 248 – 254
- [12] Song L, Chen L, Wang J, Chen F & Lan G (2017), Prediction of crystal morphology of 3, 4-Dinitro-1H-pyrazole (DNP) in different solvents. *Journal of Molecular Graphics and Modelling* 75, 62 – 70
- [13] Shi W, Chu Y, Xia M, Lei W & Wang F (2016), Crystal morphology prediction of 1,3,3-trinitroazetidine in ethanol solvent by molecular dynamics simulation. *Journal of Molecular Graphics and Modelling* 64, 94 – 100
- [14] Rohl AL (2003), Computer prediction of crystal morphology. *Current Opinion in Solid State and Materials Science* 7, 21 – 26
- [15] Shim HM, Kim JK, Kim HS & Koo KK (2014), Molecular dynamics simulation on nucleation of ammonium perchlorate from an aqueous solution. *Crystal Growth & Design* 14, 5897-5903
- [16] Zeng, JP., Bai Y-S., Chen S & Ma C-A (2013), Molecular dynamics simulation of diffusion of nitrobenzene in 3-methylimidazolium hexa fluoro phosphate ionic liquids. *Journal of Molecular Liquids* 183, 1-7
- [17] Sun Q, Liu Q, Xiao J (2014), Molecular dynamics simulation of interface interactions and mechanical properties of CL-20/HMX cocrystal and its based PBXs. *Acta Chim. Sinica* 72, 1036 –1042.
- [18] Clydesdale G, Roberts KJ, Telfer GB & Grant DJW (1997), Modeling the crystal morphology of α -lactose monohydrate. *Journal of Pharmaceutical Sciences* 86, 135 – 141
- [19] Schmidt C, Yürüdü C, Wachsmuth A & Ulrich J (2011), modeling the morphology of benzoic acid crystals grown from aqueous solution. *Crystal Engineering Communication* 13, 1159 – 1169
- [20] Coombes DS, Richard C, Catlow A, Gale JD, Rohl AL & Price SL (2005), Calculation of attachment energies and relative volume growth rates as an aid to polymorph prediction. *Crystal Growth & Design* 5, 879 – 885
- [21] Berry DJ & Steed JW (2017), Pharmaceutical cocrystals, salts and multicomponent systems; intermolecular interactions and property-based design. *Advanced Drug Delivery Reviews* 117, 3 – 24.
- [22] Zeng J, Aimin W, Xuedong G, Jingwen C, Song C & Feng X (2012), Molecular dynamics simulation of diffusion of vitamin c in water solution. *Chinese Journal of Chemistry* 30, 115 – 120
- [23] Gholizadeh R., Wang Y & Yu Y-X (2017), Molecular dynamics simulations of stability at the early stages of silica materials preparation. *Journal of Molecular Structure* 1138, 198 – 207
- [24] Shi W, Xia M, Lei W & Wang F (2014), Solvent effect on the crystal morphology of 2,6- diamino-3,5-dinitropyridine-1-oxide: a molecular dynamics simulation study. *Journal of Molecular Graphics and Modelling* 50, 71–77